

Supplementary Information

Polymorphism-induced dual phosphorescent emission from solid-state iridium(III) complex

Chang Hwan Shin,^a Jung Oh Huh,^a Min Hyung Lee*^b and Youngkyu Do*^a

^a *Department of Chemistry, KAIST, Daejeon 305-701, Republic of Korea*

^b *Department of Chemistry, University of Ulsan, Ulsan 680-749, Republic of Korea*

General Considerations. All manipulations were performed under an inert nitrogen atmosphere using standard Schlenk and glove box techniques. Anhydrous grade solvents (Aldrich) were purified by passing through an activated alumina (Acros, 50 – 200 micron) column. All reagents were used without any further purification after purchasing from Aldrich (2-Bromopyridine, 2,4-Difluorophenylboronic acid, Dibenzoylmethane, 2-Ethoxyethanol), Fluka (anhydrous Na₂CO₃), and Strem (Iridium(III) chloride hydrate). The compounds 2-(2,4-difluorophenyl)pyridine and [Ir(ppyFF)₂(μ-Cl)]₂ were prepared by a modified method of procedures reported in the literature. Deuterated solvents (Cambridge Isotope Laboratories) were dried over activated molecular sieves (5Å). ¹H and ¹³C NMR spectra of the compounds were recorded on a Bruker Spectrospin 400 spectrometer at ambient temperature. All chemical shifts are reported in δ units with reference to the residual peaks of CDCl₃ for proton (7.24 ppm) and carbon (77.0 ppm) chemical shifts. Elemental analyses (EA) were carried out on an EA1110-FISONS (CE Instruments) by the Environmental Analysis Laboratory at KAIST. MALDI-TOF-MS were measured using a Voager™ DE-STR, 4700 proteomics analyzer at Korea Basic Science Center (KBSC). UV-vis spectra were measured using a Jasco V-530 spectrophotometer. PL spectra were measured with a Spex Fluorog-3 luminescence spectrometer. PL and quantum yield measurements were performed at room temperature in a spectrophotometric grade chloroform solution. All chloroform solutions were degassed by several freeze-pump-thaw cycles using a diffusion pump. The emission quantum yield was calculated using degassed *fac*-Ir(ppy)₃ in toluene (Φ = 0.40) as a reference. Low-temperature measurements were recorded in 5 mm diameter quartz tubes that were placed in a quartz-walled Dewar flask filled with liquid nitrogen (77 K). Emission lifetimes were determined using a Third Harmonic of ND:YAG laser (Spectra-Physics LAB170, 10Hz). A laser sampled by a fused silica window was applied to excite the sample, and delay time (310 μs) between flash lamp and Q-switch was used to reduce the laser output power. The final power of the laser to the pump samples was about 100 μJ/pulse. A monochromator (Dongwoo Optron, DM150i) and a general Photo Multiplier Tube (Hamamatsu, R928) were employed to select the wavelength of the emission and to detect the strength of the emission. The signals from the PMT were spread on an oscilloscope (Lecroy waverunner 104Xi, 1GHz bandwidth) and recorded. Cyclic voltammetry was performed using an AUTOLAB/PGSTAT12 model system with a three-electrode cell under a nitrogen atmosphere. Anhydrous acetonitrile was used as the solvent and 0.1 M tetrabutylammonium hexafluorophosphate was used as the supporting electrolyte.

A Pt wire was used as the counter electrode, and an Ag/AgNO₃ (0.1 M in acetonitrile) electrode as the reference electrode. The working electrode was a Pt wire and redox potentials were recorded at a 50 mVs⁻¹ scan rate. The redox potentials were reported against the ferrocene/ferrocenium (Cp₂Fe/Cp₂Fe⁺) redox couple that was used as an internal standard.

Synthesis of Ir(ppyFF)(DBM) (1). [Ir(ppyFF)₂(μ-Cl)]₂ (2.35 g, 1.93 mmol), dibenzoylmethane (1.30 g, 5.79 mmol), and Na₂CO₃ (2.05 g, 19.3 mmol) were mixed in 2-ethoxyethanol (30 mL) at room temperature. The mixture was stirred and heated at reflux overnight under a N₂ atmosphere. After cooling to room temperature, water (30 mL) was added, and the mixture was then filtered to give a dark crude product. The crude product was washed with water (30 mL) and ether (30 mL). The pure complex was obtained by flash chromatography on a silica column using dichloromethane as an eluent to yield **1** as a yellow solid (1.90 g, 62%). ¹H NMR (400.13 MHz, CDCl₃, ppm): δ 8.51 (d, *J* = 4.8 Hz, 2H), 8.24 (d, *J* = 8.4 Hz, 2H), 7.78 (td, *J* = 7.2, 1.2 Hz, 4H), 7.73 (t, *J* = 7.5 Hz, 2H), 7.42 (t, *J* = 7.3 Hz, 2H), 7.31 (t, *J* = 7.6 Hz, 4H), 7.08 (td, *J* = 6.6, 1.2 Hz, 2H), 6.59 (s, 1H), 6.38 (td, *J* = 11, 2.3 Hz, 2H), 5.76 (dd, *J* = 8.8, 2.3 Hz, 2H). ¹³C NMR (100.62 MHz, CDCl₃, ppm): δ 179.27, 165.31, 165.24, 163.92, 163.79, 162.12, 161.99, 161.38, 161.26, 159.55, 159.42, 151.64, 151.58, 148.00, 140.71, 137.96, 130.56, 128.79, 128.75, 128.36, 126.86, 122.66, 122.47, 121.71, 115.31, 115.28, 115.15, 115.12, 97.49, 97.22, 96.95, 94.98. MALDI-TOF-MS: *m/z* = 795.79 (M⁺). Anal. Calcd. for C₃₇H₂₃F₄IrN₂O₂: C 55.84, H 2.91, N 3.52; Found: C 56.07, H 2.62, N 3.51.

X-ray Crystallography. Single crystals of **1A** and **1B** obtained from THF/*n*-hexane solutions were coated with Paratone oil and diffraction data were measured at 100 K with synchrotron radiation ($\lambda = 0.74999 \text{ \AA}$) on a 4AMXW ADSC Quantum-210 detector equipped with a silicon double crystal monochromator at Pohang Accelerator Laboratory in Korea. The reflection data were collected as π scan frames with a width of 1°/frame and an exposure time of 1 s/frame. HKL2000 (Ver. 0.98.698) was used for data collection, cell refinement, reduction, and absorption correction. The structure was solved by direct methods and refined by full-matrix least-squares methods using the SHELXTL program package with anisotropic thermal parameters for all non-hydrogen atoms. Hydrogen atoms were placed at their geometrically calculated positions and refined riding on the corresponding carbon atoms with isotropic thermal parameters.

Table S1. Crystallographic data and parameters for **1A** and **1B**.

Complexes	1A (orange red)	1B (yellow)
formula	(C ₃₇ H ₂₃ F ₄ IrN ₂ O ₂)·(C ₄ H ₈ O) _{0.5}	C ₃₇ H ₂₃ F ₄ IrN ₂ O ₂
formula weight	831.84	795.79
crystal system	Monoclinic	Triclinic
space group	<i>C2/c</i>	<i>P</i> -1
<i>a</i> (Å)	23.963(5)	11.745(2)
<i>b</i> (Å)	19.684(4)	16.325(3)
<i>c</i> (Å)	27.110(5)	17.965(4)
α (°)	90	113.67(3)
β (°)	94.00(3)	107.93(3)
γ (°)	90	94.38(3)
<i>V</i> (Å ³)	12756(4)	2921.4(10)
<i>Z</i>	16	4
ρ_{calc} (g cm ⁻³)	1.733	1.809
μ (mm ⁻¹)	4.251	4.635
<i>F</i> (000)	6528	1552
<i>T</i> (K)	100(2)	100(2)
<i>hkl</i> range	-20→33, -21→28, -39→38	-13→0, -17→17, -19→20
no. of reflns measd	36083	7817
no. of unique reflns [<i>R</i> _{int}]	19220 (0.0358)	7817 (0.0000)
no. of refined parameters	874	829
<i>R</i> 1 ^a , <i>wR</i> 2 ^b (<i>I</i> > 2σ(<i>I</i>))	0.0427, 0.1186	0.0709, 0.2075
GOF on <i>F</i> ²	1.000	1.003
ρ_{fin} (max/min) (e Å ⁻³)	3.862/-4.137	2.372/-4.367

^a $R1 = \sum ||F_o| - |F_c|| / \sum |F_o|$. ^b $wR2 = \{[\sum w(F_o^2 - F_c^2)^2] / [\sum w(F_o^2)^2]\}^{1/2}$.

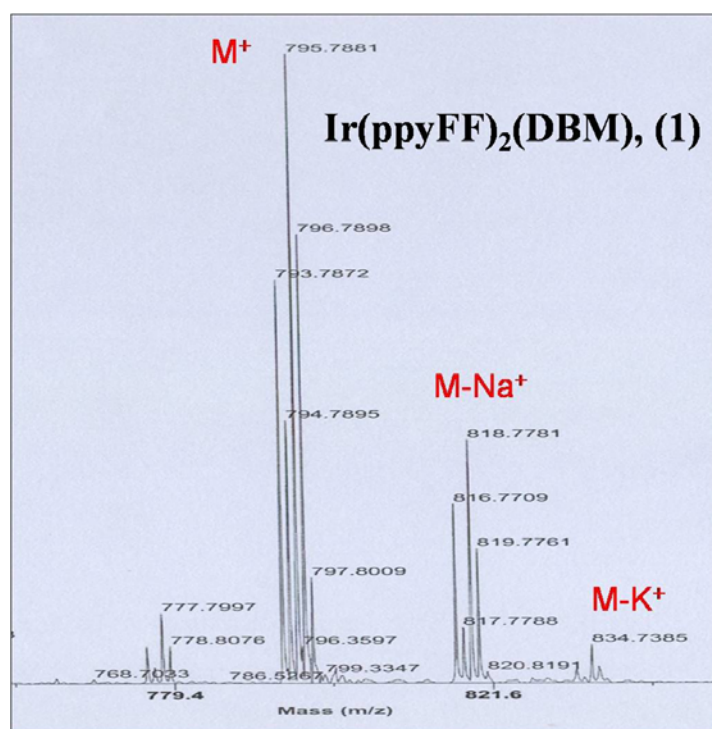


Fig. S1. MALDI-TOF-MS spectrum of **1**

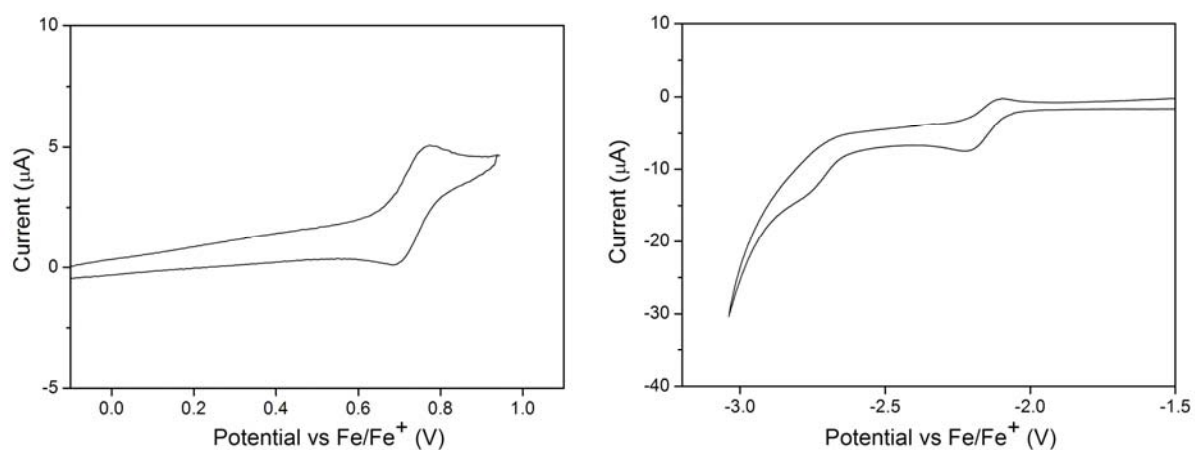


Fig. S2. Cyclic voltammograms of **1** showing oxidation (left; $E_{\text{ox}}(\text{rev}) = 0.73$ V) and reduction (right; $E_{\text{red}}^{\text{1st}}(\text{rev}) = -2.16$ V and $E_{\text{red}}^{\text{2nd}}(\text{irrev}) = -2.77$ V).

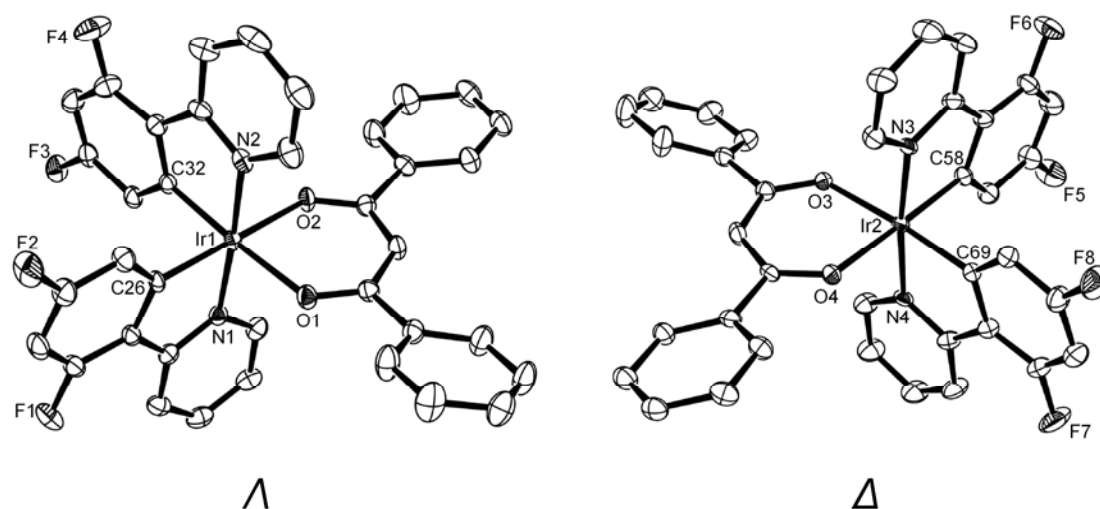


Fig. S3. Molecular structures of Λ - (left) and Δ -isomers (right) of **1A** (50% ellipsoid). The H-atoms and THF molecule were omitted for clarity. Selected bond distances (\AA) and angles (deg): Ir1–C26 1.991(4), Ir1–C32 1.996(4), Ir1–N1 2.041(4), Ir1–N2 2.034(4), Ir1–O1 2.130(3), Ir1–O2 2.148(3), Ir2–C58 1.997(4), Ir2–C69 1.974(4), Ir2–N3 2.035(4), Ir2–N4 2.037(4), Ir2–O3 2.141(3), Ir2–O4 2.134(3), C26–Ir1–C32 85.22(17), C32–Ir1–N2 80.05(17), C26–Ir1–N1 80.55(18), C26–Ir1–O1 92.39(15), C32–Ir1–O2 95.20(15), O1–Ir1–O2 87.52(13), C58–Ir2–C69 88.47(18), C58–Ir2–N3 80.92(17), C69–Ir2–N4 80.67(17), C69–Ir2–O4 90.14(15), C58–Ir2–O3 93.81(16), O3–Ir2–O4 87.88(12).

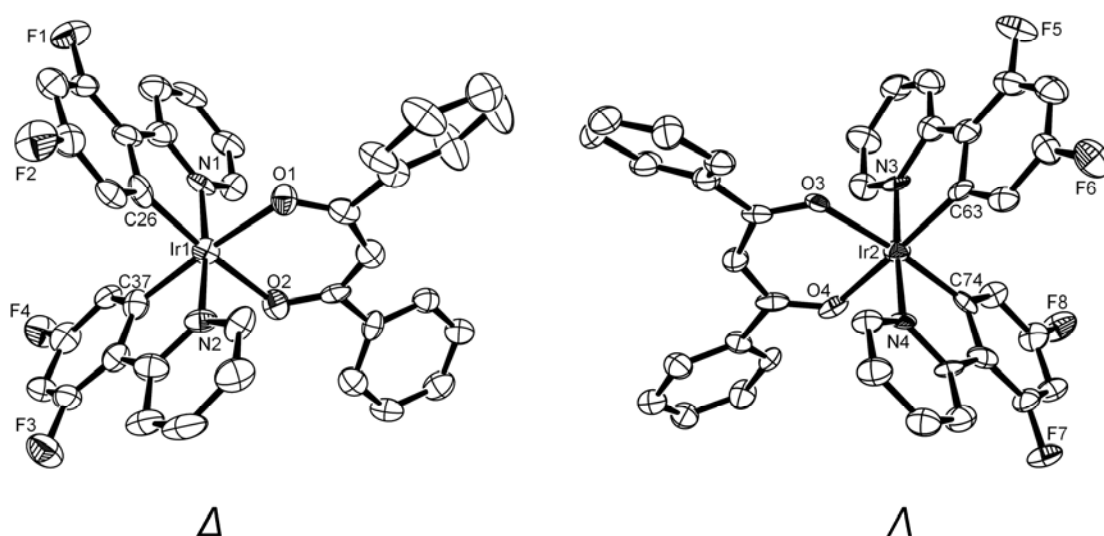


Fig. S4. Molecular structures of Δ - (left) and Λ -isomers (right) of **1B** (50% ellipsoid). The H-atoms were omitted for clarity. Selected bond distances (Å) and angles (deg): Ir1–C26 1.979(13), Ir1–C37 1.983(10), Ir1–N1 2.057(8), Ir1–N2 2.025(8), Ir1–O1 2.132(6), Ir1–O2 2.156(8), Ir2–C63 1.980(10), Ir2–C74 1.974(9), Ir2–N3 2.040(8), Ir2–N4 2.046(8), Ir2–O3 2.134(6), Ir2–O4 2.090(7), C26–Ir1–C37 91.0(4), C37–Ir1–N2 80.8(4), C26–Ir1–N1 81.4(4), C26–Ir1–O1 89.6(3), C37–Ir1–O2 91.1(3), O1–Ir1–O2 89.0(3), C63–Ir2–C74 91.4(3), C63–Ir2–N3 80.6(4), C74–Ir2–N4 81.6(3), C74–Ir2–O4 87.8(3), C63–Ir2–O3 91.8(3), O3–Ir2–O4 89.7(2).

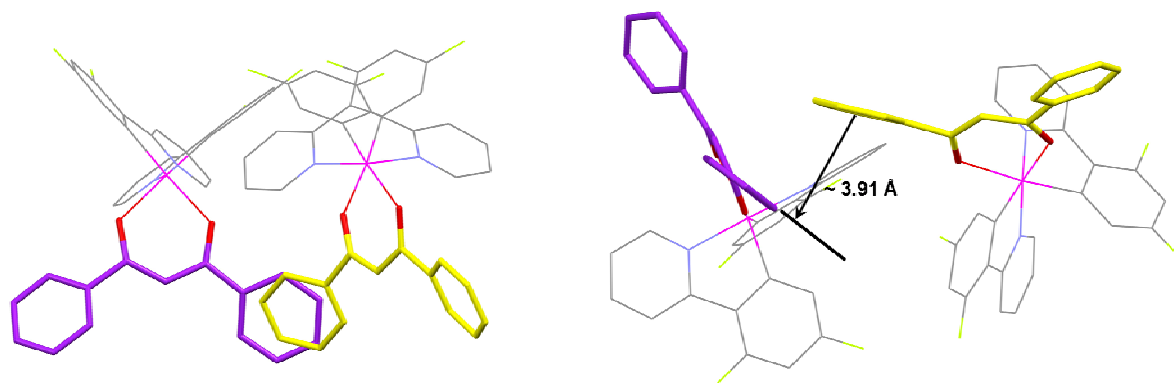


Fig. S5. Crystal packing diagrams of yellow crystal **1B** showing a spatial arrangement of the DBM moieties.

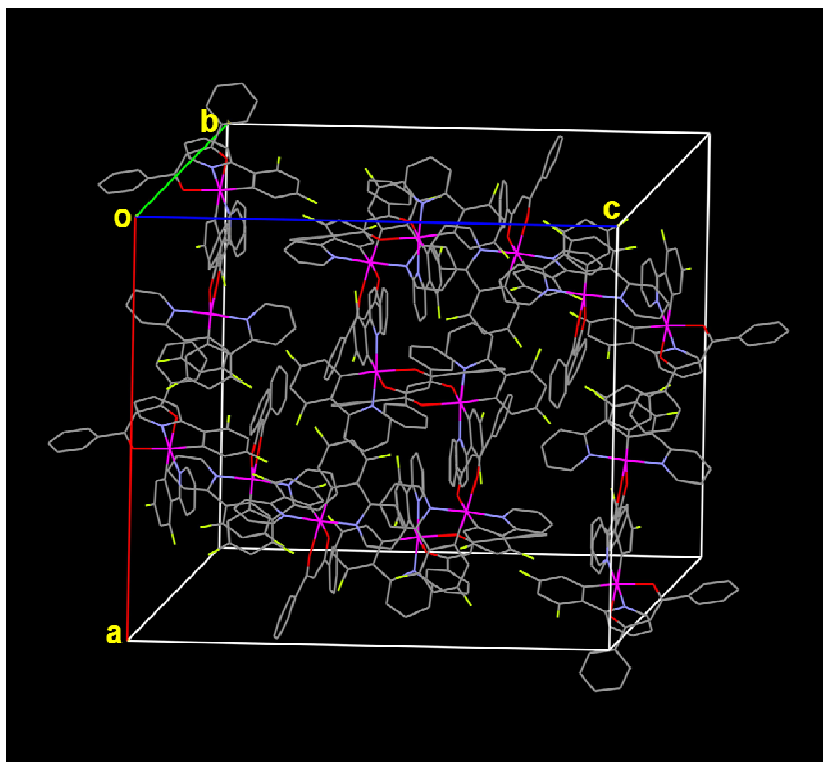


Fig. S6. Unit cell packing diagram of orange red crystal (**1A**).
The disordered THF molecules were omitted for clarity.

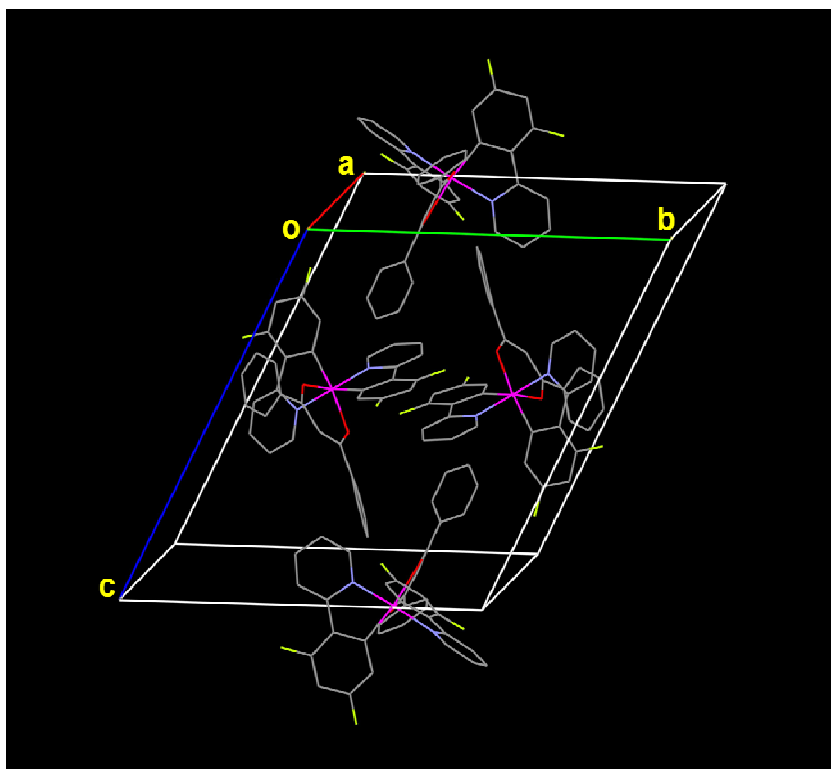


Fig. S7. Unit cell packing diagram of yellow crystal (**1B**).

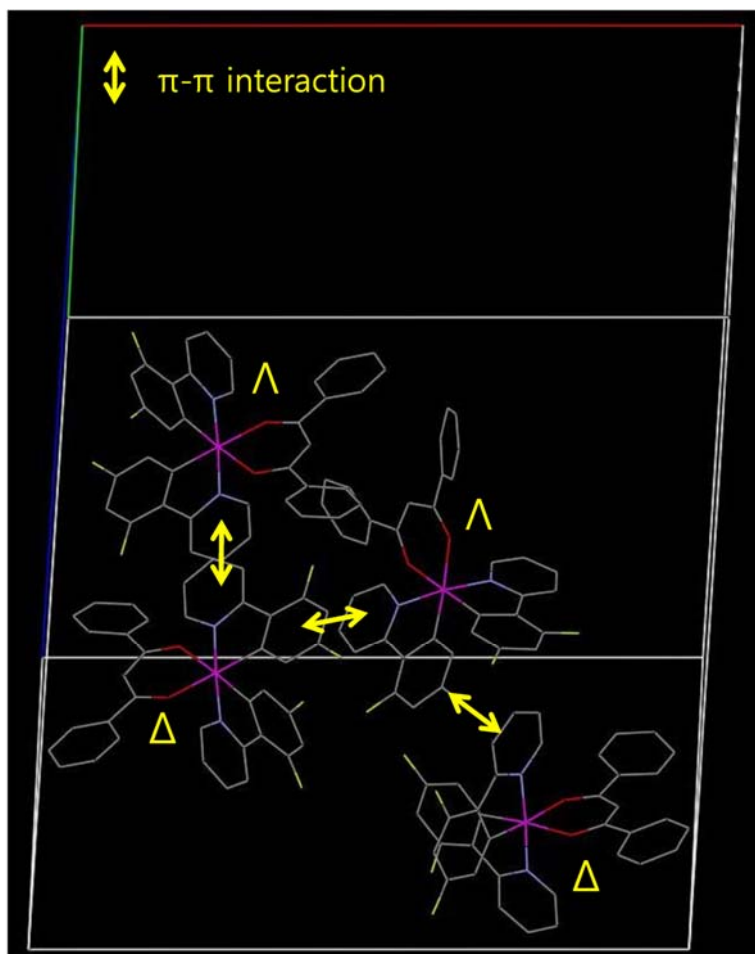


Fig. S8. π - π interactions (**LLLL** interactions in Fig 4a) between Δ - and Λ -stereoisomers in the crystal packing structure of orange red crystal (**1A**). The other 12 molecules in the unit cell were omitted for clarity.

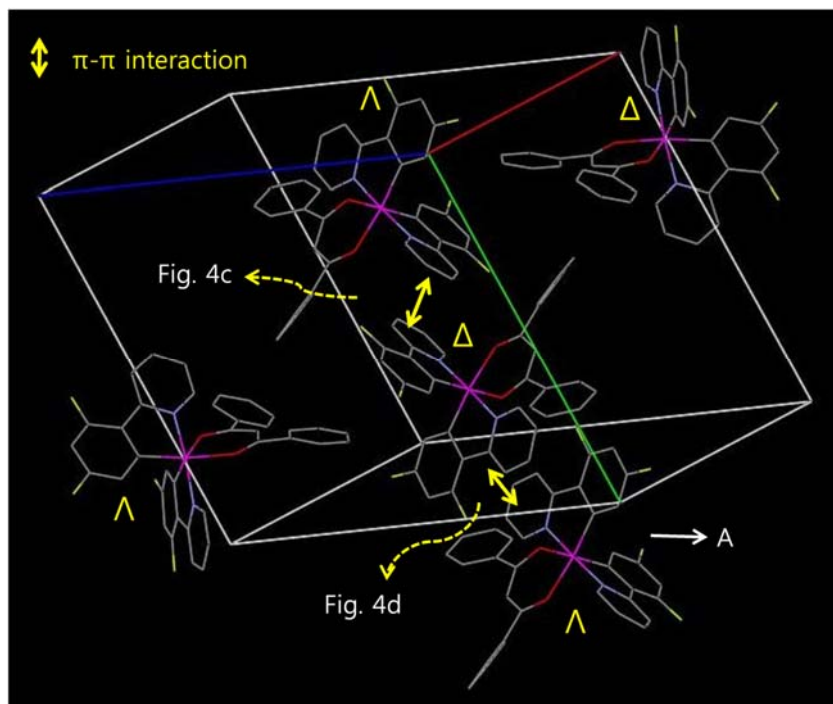


Fig. S9. π - π interactions (**LL** interactions in Fig 4c and 4d) between Δ - and Λ -stereoisomers in the crystal packing structure of yellow crystal (**1B**) (the molecule **A** from an adjacent unit cell).